Constructing the Universe with Clusters of Galaxies, IAP 2000 meeting, Paris (France) July 2000
Florence Durret & Daniel Gerbal eds.

TESTING STRUCTURE EVOLUTION MODELS AND MEASURING DISTANCES WITH INTERMEDIATE REDSHIFT GALAXY CLUSTERS

Joseph J. Mohr[1,2], Erik D. Reese[2], E. Ellingson[3], Aaron D. Lewis[3], August E. Evrard[4]
[1] *Departments of Astronomy and Physics, University of Illinois, Urbana, IL 61801 USA*
[2] *Department of Astronomy and Astrophysics, University of Chicago, Chicago, IL 60637 USA*
[3] *Department of Astronomy, University of Colorado, Boulder, CO 80309 USA*
[4] *Departments of Physics and Astronomy, University of Michigan, Ann Arbor, MI 48109 USA*

Galaxy clusters in the nearby universe exhibit evidence for regularity on the scale of their virial regions, which is comparable to the regularity in elliptical galaxies. We review observations of the X-ray isophotal Size-Temperature (ST) relation in the nearby universe, and then we examine an ensemble of clusters at intermediate redshift. We show– using archival ROSAT HRI data– that the 11 CNOC clusters with measured ICM temperatures exhibit a ST relation with slope and scatter consistent with the local relation. Using the canonical structure formation model, we argue that the ST relation normalization is not expected to evolve with redshift, making it a potentially interesting distance indicator. We show that the observed intermediate redshift ST relation normalization excludes the $\Omega_M = 1$ model, but is consistent with the $\Omega_M = 0.3$ and $\Omega_\Lambda = 0.7$ model.

1 Introduction

Galaxy cluster scaling relations provide insights into the details of structure formation on cluster scales. The scatter about the X-ray ST relation[1] in a large, flux limited cluster ensemble[2] is 15%, comparable to the scatter of elliptical galaxies around the Fundamental Plane[3]. This fact stands in sharp contrast to the large scatter in the X-ray luminosity-temperature (LT) relation[4]. A consistent interpretation is that galaxy clusters are regular objects on the scale of their virial regions, but that cooling instabilities which occur in the core can significantly bias their luminosities (but only slightly bias their emission weighted mean temperatures). The interpretation is supported by a study of the LT relation in a cluster ensemble constructed to contain no clusters with central cooling instabilities[5].

The ST relation is an important tool for studying the formation history of galaxy clusters. The scatter about the ST relation is sufficiently low that it rules out models of structure formation where the initial distribution of density perturbations is non-Gaussian[6]. The slope of the ST relation is steeper than the expectation from standard structure formation models; this steepness can be explained if the intracluster medium (ICM) has some other source of heat besides the shocking and compressional heating during cluster formation. In fact, the local ST relation, LT relation and the ICM mass-temperature relation can all be explained with a particular level of early preheating[7]. Scaling relation measurements at a range of redshifts will allow us to test preheating models and perhaps even determine the epoch of preheating.

Here we present new measurements of the local ST relation and describe the first measurements of the ST relation at intermediate redshift. Many of the results summarized here are presented in full detail in a Mohr et al. (2000)[8] paper in *The Astrophysical Journal.*

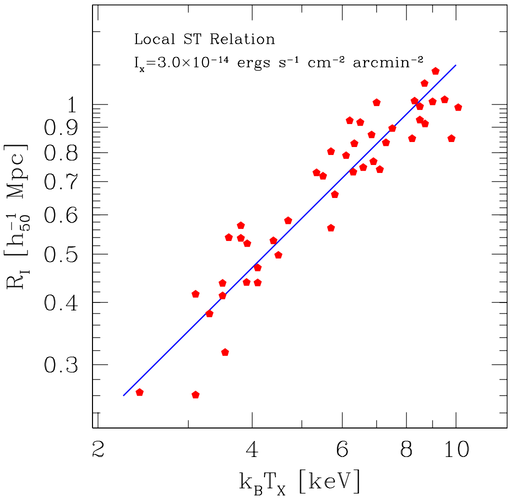

Figure 1: The X-ray isophotal size versus emission weighted mean ICM temperature T_X for an X-ray flux limited sample of 45 nearby clusters. We use the isophote $I = 3.0 \times 10^{-14}$ erg s^{-1} cm^{-2} arcmin^{-2} within the cluster rest frame 0.5:2.0 keV band. The solid line represents the best fit relation, and the RMS scatter about this line is 15% in size.

2 Local Size-Temperature Relation

Figure 1 contains a plot of the best fit ST relation for a flux limited ensemble of 45 galaxy clusters. We plot the cluster emission weighted mean ICM temperature (taken from the literature) versus X-ray isophotal size. This isophotal size is measured directly (i.e. non-parametrically) from the ROSAT PSPC images using the isophote $I = 3.0 \times 10^{-14}$ erg s^{-1} cm^{-2} arcmin^{-2} within the cluster rest frame 0.5:2.0 keV band. As already mentioned, the scatter about this best fit relation is 15% in size. Many of the famous cluster merger candidates like A 754, COMA, A 2319 and A 3667 appear as outliers in this ensemble. Because the evidence for cluster growth at the present epoch is overwhelming[9,10,11], this evidence for regularity probably suggests that, on average, clusters grow through small scale mergers which don't perturb them significantly from their equilibrium state, and that the relaxation timescales required for them equilibrate after a merger are short compared to the timescales between mergers. If the same situation were to hold at intermediate redshift, then we would expect to observe an ST relation there with similar scatter.

3 Intermediate Redshift Size-Temperature Relation

We study the intermediate redshift ST relation using the CNOC ensemble of galaxy clusters[12,13]. In particular, we analyze the ROSAT HRI images of the 11 members of the CNOC sample with available emission weighted mean ICM temperatures. Because the quality of these images is much lower, on average, in our intermediate sample than in our local sample, we measure isophotal sizes parametrically. We fit circular β models to the images, and then determine the range of apparent isophotal size which is consistent with the data. A table of best fit parameters and uncertainties appears elsewhere[8]. We use the same isophote that we used in the local sample–

specifically, $I = 3.0 \times 10^{-14}$ erg s^{-1} cm^{-2} arcmin^{-2} within the cluster rest frame 0.5:2.0 keV band.

We convert from apparent isophotal size to physical size using the angular diameter distance. Angular diameter distances require the cluster redshift and an assumption about the cosmological parameters. Figure 2 is the resulting ST relation at intermediate redshift when we assume $\Omega_M = 0.3$ and $\Omega_\Lambda = 0.7$. The dashed line is the best fit relation for this sample, and the solid line is the best fit relation for the local sample (Fig 1). The slope, scatter and zeropoint of this intermediate redshift relation is consistent with the local sample. Of course, with such a small sample the scatter isn't well constrained.

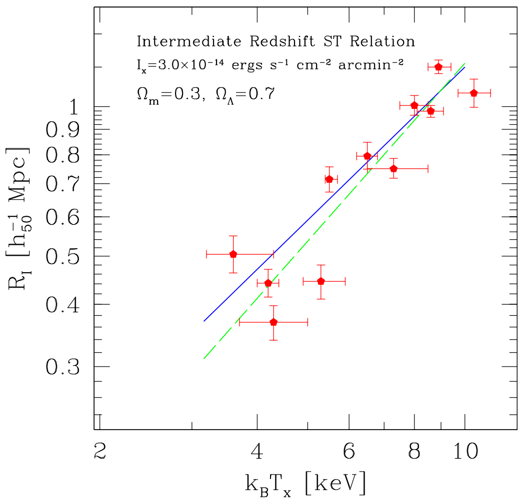

Figure 2: The X-ray ST relation for 11 members of the CNOC cluster sample with measured T_X. For this figure the conversion from measured $\theta_I \to R_I$ is done assuming $\Omega_M = 0.3$ and $\Omega_\Lambda = 0.7$. Error bars denote 1 σ uncertainties in emission weighted mean temperature T_X and in isophotal size R_I. The solid line is the best fit ST relation determined from the nearby cluster sample (Fig 1), and the dashed line is the best fit ST relation for the intermediate redshift sample.

The canonical structure formation model[8,14] would lead us to expect that the ST relation does not evolve with redshift. As shown in Figure 2, if the true cosmology is $\Omega_M = 0.3$ and $\Omega_\Lambda = 0.7$, this evolution expectation is consistent with the observations.

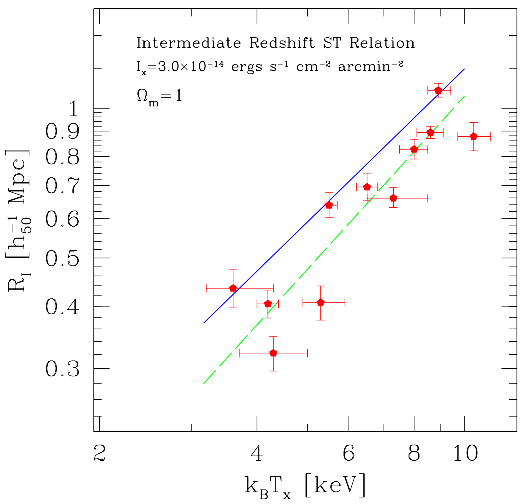

Figure 3: The X-ray ST relation for 11 members of the CNOC cluster sample. For this figure the conversion from measured $\theta_I \to R_I$ is done assuming $\Omega_M = 1$. Error bars denote 1 σ uncertainties in emission weighted mean temperature T_X and in isophotal size R_I. The solid line is the best fit ST relation determined from the nearby cluster sample (Fig 1), and the dashed line is the best fit ST relation for the 11 intermediate redshift clusters.

We can turn this argument around, assume that the standard evolution model is correct and then use the ST relation measurements to constrain cosmological parameters. Figure 3 is a plot of the intermediate redshift ST relation under the assumption that $\Omega_M = 1$. As in Figure 2, the dashed line is the best fit relation, and the solid line is the local relation. The slope and scatter are approximately independent of these cosmological parameters. Figures 2 and 3 make it clear that low Ω_M universes are more consistent with these data. In fact, we've examined a broad range of cosmological models and used these data to estimate their likelihoods[8]. The results are broadly consistent with constraints from comparison of local and high redshift SNe Ia[15,16]. With only 11 distance measurements, the ST relation constraints are significantly weaker than those from SNe Ia.

4 Future Work

The intermediate and high redshift cluster data being accumulated by Chandra and XMM-Newton will allow a far more constraining study of the evolution of the ST relation. My collaborators and I are beginning a study of over 40 clusters in the Chandra archive, and our primary goal is to use cluster scaling relations to test structure evolution models. If these higher quality data support the canonical structure evolution model, then we plan to use the ST relation to measure relative distances and constrain cosmological parameters.

Acknowledgments

We thank the organizers– especially Florence Durret– for a delightfully stimulating conference. JJM is a Chandra Fellow supported by grant PF8-1003, awarded through the Chandra Science Center. The Chandra Science Center is operated by the Smithsonian Astrophysical Observatory for NASA under contract NAS8-39073. EDR is supported by NASA GSRP Fellowship NGT5-50173. EE acknowledges support provided by the National Science Foundation grant AST 9617145. AEE acknowledges support from NSF AST-9803199 and NASA NAG5-8458. This research has made use of data obtained through the High Energy Astrophysics Science Archive Research Center Online Service, provided by the NASA/Goddard Space Flight Center.

References

1. Mohr, J.J. & Evrard, A.E. *ApJ* **491**, 13 (1997).
2. Edge, A.C., Stewart, G.C., Fabian, A.C. & Arnaud, K.A. *MNRAS* **245**, 559 (1990).
3. Jørgensen, I., Franx, M. & Kjærgaard, P. *MNRAS* **280**, 167 (1996).
4. David, L.P., Slyz, S.C., Forman, W., Vrtilek, S.D. & Arnaud, K.A. *ApJ* **412**, 479 (1993).
5. Arnaud, M. & Evrard, A.E. *MNRAS* **305**, 631 (1999).
6. Verde, L., Kamionkowski, M., Mohr, J.J. & Benson, A. *MNRAS* , (submitted)
7. Bialek, J., Evrard, A.E. & Mohr, J.J. *ApJ* , (submitted).
8. Mohr, J.J., Reese, E.D., Ellingson, E., Lewis, A.D. & Evrard, A.E. *ApJ* **544**, (2000)
9. Geller, M.J. & Beers, T.C. *PASP* **94**, 421 (1982).
10. Dressler, A. & Shectman, S.A. *AJ* **95**, 284 (1988)
11. Mohr, J.J., Evrard, A.E., Fabricant, D.G & Geller, M.J. *ApJ* **447**, 8 (1995).
12. Yee, H.K.C., Ellingson, E., & Carlberg, R.G. *ApJ Supp* **102**, 269 (1996).
13. Lewis, A.D., Ellingson, E., Morris, S.L. & Carlberg, R.G. *ApJ* **517**, 587 (1999).
14. Bryan, G.L. & Norman, M.L. *ApJ* **496**, 80 (1998).
15. Schmidt, B.P. *et al.* *ApJ* **507**, 46 (1998).
16. Perlmutter, S. *et al.* *ApJ* **517**, 565 (1999).